Gear Failure Analysis Involving Grinding Burn

G. Blake, M. Margetts and W. Silverthorne

Management Summary

When gears are case-hardened, it is known that some growth and redistribution of stresses that result in geometric distortion will occur. Aerospace gears require post case-hardening grinding of the gear teeth to achieve necessary accuracy. Tempering of the case-hardened surface, commonly known as grinding burn, occurs in the manufacturing process when control of the heat generation at the surface is lost. Excessive heat generated at the surface can induce surface tempering and/or reaustenitize the surface in a localized area. The localized area will have reduced or altered mechanical properties in addition to an unfavorable residual stress state (Ref. 1).

Linear cracks along the dedendum of the working gear tooth face were found in three adjacent teeth during visual inspection of a gearbox. No teeth had been liberated. A detailed inspection of the gearbox found no other components with distress.

Metallurgical evaluation determined that the cracks initiated at the boundary of a localized grinding burn, which had reaustenitized. The cracks propagated inward from the tooth surface in fatigue to a depth greater than the depth of the case.

The metallurgical evaluation could not conclude if the crack trajectory would propagate across the tooth cross section or radially into the gear rim. A cross section trajectory results in the liberation of teeth. Linear elastic fracture mechanics (LEFM) analysis was then used to predict the cracks' future propagation path based on assumptions from the one subject gear.

The subject gear was processed for grinding burn using an ammonium persulfate etch solution. A design of experiments was conducted to understand the effects of the factors and interactions that impact the capability of the ammonium persulfate process used in production to detect grinding burn.

Presented are the metallurgical findings, load distribution analysis of actual geometry, crack propagation analysis, and design of experiment results of the ammonium persulfate etch process.

Overview of Gear System

The subject gearbox had accumulated 1,650 hours of use at the time of inspection. A partial illustration of the gear train and the gear is shown in Figure 1. The gear and mating pinion are carburized, ground and shot peened AMS6265. The engine torque path is also shown in Figure 1.

Background

The gearbox has a chip detector in the scavenge oil passage. The technicians removed the chip detector and found a large sliver of material clinging to the end. The size of the sliver is shown in Figure 2.

Typically, wearing or pitting components will generate very fine particles that, when mixed with oil, create a paste. The paste is what most technicians expect to find when investigating a chip light indication. The size of the debris found on the plug was cause for removal of the gearbox.

Tear-Down Inspection

Cracks were found in the first-stage spur gear as shown in Figure 3. Tooth number eight, shown in Figure 3, was found to have a divot close in size to the metallic sliver found on the chip detector. The cracks were located in three adjacent teeth on the driven side. The cracks stretched across the central 75% of the face width within the active tooth profile. The cracks were arc shaped, higher on the active tooth profile at the ends than in the center.

The visual cracks and distress of the gear were confined to the three teeth shown in Figure 3. The remainder

of the gear teeth showed no evidence of distress.

A detailed inspection was performed on all other parts of the gearbox. No other components showed any signs of degradation or indications of high load experience. The mating pinion gear showed no signs of surface distress or maldistributed load as shown in Figure 4.

Magnetic particle inspection (MPI) was performed on the subject gear at the manufacturer. No cracks, in addition to those found visually, were found. No etch inspection was performed at this time to prevent altering the crack surfaces, as the cracks were to be evaluated in detail as part of the destructive metallurgical investigation.

Inspection of the pinion and subject gear tooth geometry was performed. The geometry of both members was within specification and was of high quality.

Metallurgical Evaluation

A photographic montage through the crack on tooth 6 (see Figure 3) is presented in Figure 5. The crack was approximately 0.103" long and 0.061" in depth. Several smaller cracks were observed branching from the main crack. The crack intersected the surface at approximately 0.23" from the tooth tip.

Figure 5 shows the crack trajectory to be inward from the tooth surface. Analysis will be presented in the later portion of this paper to bound the crack propagation path.

The cross section was etched as shown in Figure 6 and grinding abuse was observed on both sides of the tooth. Detailed views of the grinding abuse are shown in Figures 7 and 8. The grinding abuse produced a rehardened layer on the surface measuring up to 0.007" deep. The crack followed the heat-affected zone, as illustrated in the upper image in Figure 7.

Similar grinding abuse was observed on the coast side of the tooth, as shown in Figure 8. The dotted lines in Figure 8 show the approximate location of the five hardness surveys. The hardness was reduced in the over-

continued

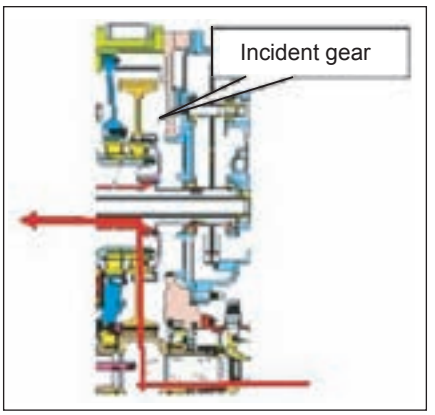

Figure 1—Partial illustration of gear train showing torque path.

Figure 2—Debris found on chip detector.

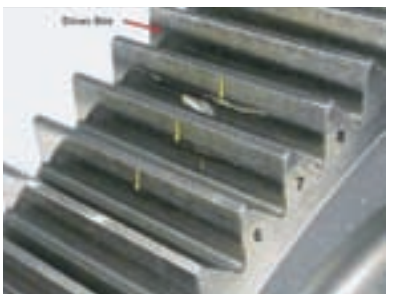

Figure 3—Three adjacent teeth cracked observable without MPI or magnification.

Figure 4—Mating pinion showing no surface distress or evidence of maldistributed load.

Figure 5—Photo montage of crack from tooth surface.

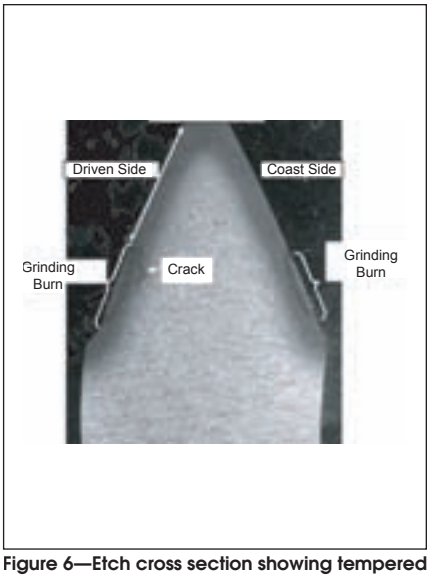

Figure 6—Etch cross section showing tempered and rehardened (burned) zone in dedendum area of the driven and coast side of the gear tooth.

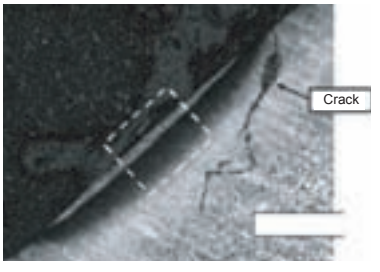

Figure 7—Detailed views of the grinding abuse and crack on the driven side. Etchant 5% Nital.

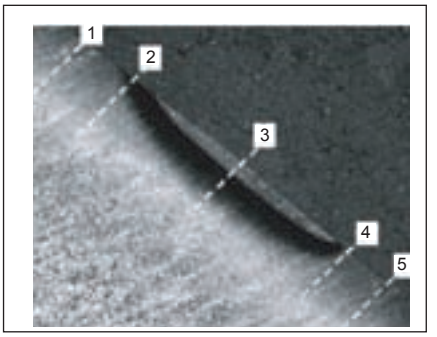

Figure 8—Coast side showing rehardened and tempered zone and locations of hardness traverses.

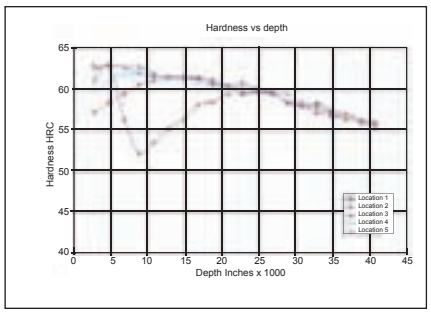

Figure 9—Hardness vs. depth at locations with and outside of the rehardened zone.

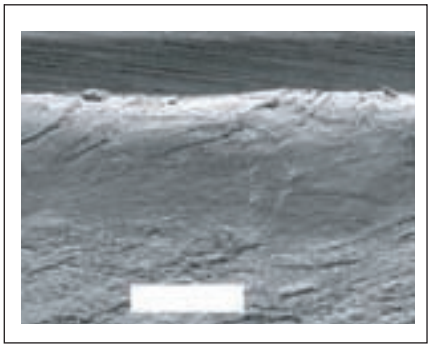

Figure 10—SEM photo showing fatigue direction from mid face towards end face.

Table 1—AGMA Index MOS

	MOS
Bending	1.30
Contact	1.10
Flash Temperature	1.08

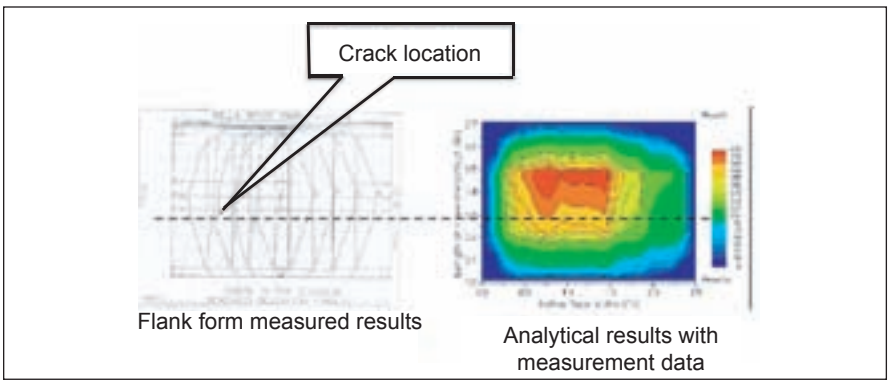

Figure 11—Approximate crack location vs. contact stress distribution.

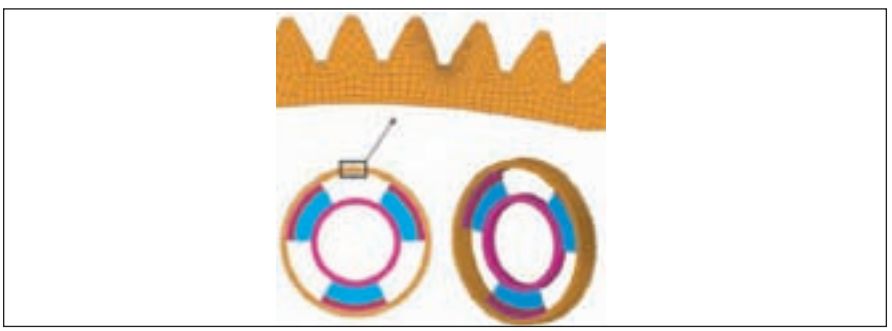

Figure 12—2D FEA model of incident gear with tooth geometry.

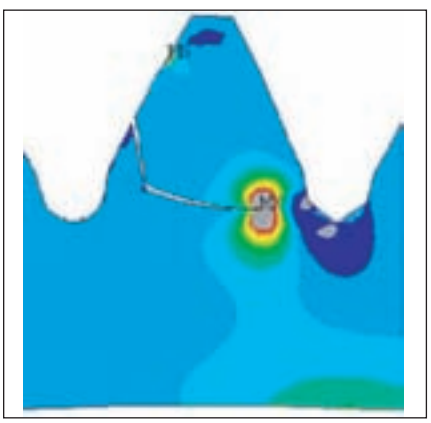

Figure 13—Crack trajectory solution starting from initial crack using maximum continuous torque and speed – first principal stress contours shown.

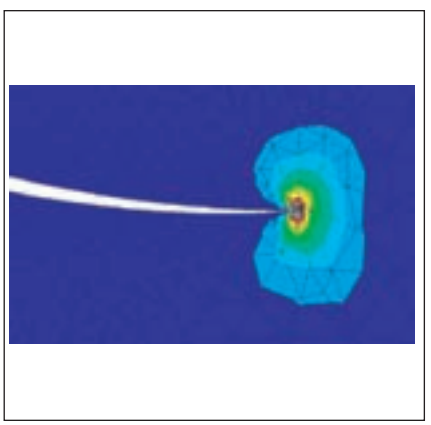

Figure 14—Quarter-point rosette used to model crack tip.

tempered areas (dark colored zone), as shown in Figure 9.

The No. 6 gear tooth section was laboratory-fractured to expose the crack surface. The crack could not be completely opened due to its shallow depth and orientation. A SEM (scanning electron microscope) photograph of the fracture is shown in Figure 10. The crack morphology was indicative of fatigue progression from mid face towards end face, as illustrated in Figure 10. The arrows indicate the direction of local fatigue crack progression.

Analysis

Analysis was performed to understand the location, shape and expected crack trajectory. A crack trajectory that results in the ejection of a single tooth or multiple teeth has a different end result than one that propagates into the gear blank.

The flank form inspection of the incident gear located the approximate radial position of the crack. The profile traces were made at the mid face of each tooth. The profile chart shown in Figure 11 shows four adjacent teeth, three of which contain the cracked teeth. The approximate location of the crack is shown as a rapid change (bump) in the lower 25% of the profile chart.

Load distribution vs. crack location. *Load Distribution Program version 10.9* was used to predict the gear load distribution. The actual measured geometry of the pinion and incident gear was input.

The contact stress distribution of the gear relative to the approximate crack location is shown in Figure 11. The crack location is near the start of single-tooth contact of the gear but not in the area of highest contact stress. However, the crack seems to follow the contour of the surface stress in the axial direction.

The margin of safety (MOS), using the AGMA index method, was greater than 1.0, as shown in Table 1. None of the AGMA index MOS would suggest premature crack initiation.

Crack trajectory analysis. Analysis was performed to predict the crack trajectory. A 2D finite element model (FEA) with actual tooth geometry was

created as shown in Figure 12.

The crack as measured in Figure 5 was added to the model. Linear elastic fracture mechanics (LEFM) was then used to predict the crack trajectory from this initial point. The solution is shown in Figure 13. The crack tip was modeled as a quarter-point rosette, as shown in Figure 14. The solution shown represents maximum continuous speed and maximum continuous torque applied at the highest point of single tooth contact.

The depth of the initial crack depth is slightly below the case-core transition point. The model assumed no residual stress in this area of the gear.

The model was then used to predict the effects of speed on crack trajectory. Reference 2 highlights the effects of rotational speed on crack trajectory. At maximum continuous speed, the crack trajectory was across the tooth. The trajectory changed toward the blank center as speed increased, given the same applied torque (Figure 15).

Published analytical and test results in References 2–4 were used to validate the model. Reference 5 highlights the effects of rim thickness on the alternating stress range experienced in the gear tooth root. The supporting geometry is therefore expected to have a strong influence on crack trajectory.

Etch Inspection Design of Experiments

A design of experiments (DOE) was conducted to understand the effects of the factors and interactions that impact the capability of the ammonium persulfate process to detect grinding burn.

The DOE was a full factorial with replication, two levels per factor, with center point. The variables were % ammonium persulfate and % HCL. The response variable was burn indication (faint, light, dark).

The etch process was replicated in the Failure Analysis Laboratory as shown in Figure 16. The process steps for the DOE are shown in Table 2.

The maximum observed concentration levels were used as upper

continued

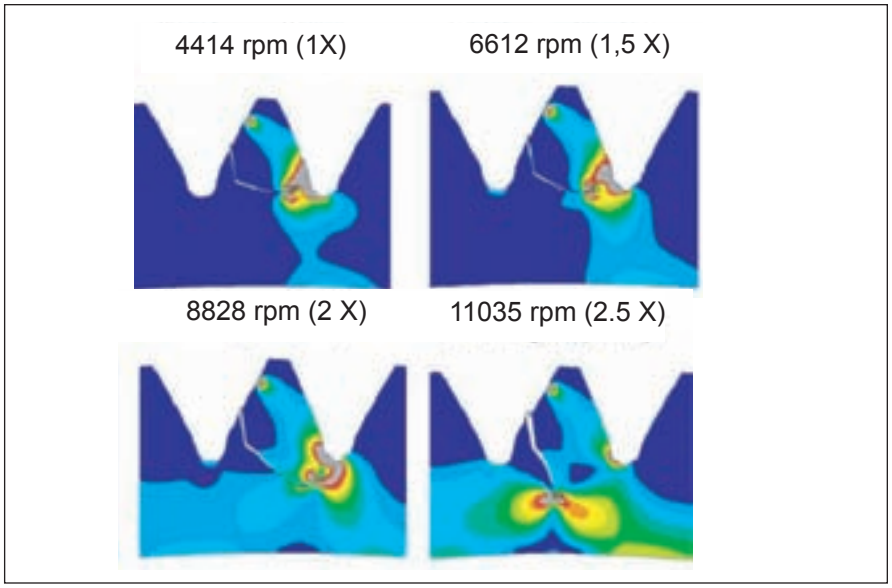

Figure 15—Crack trajectory vs. rotational speed.

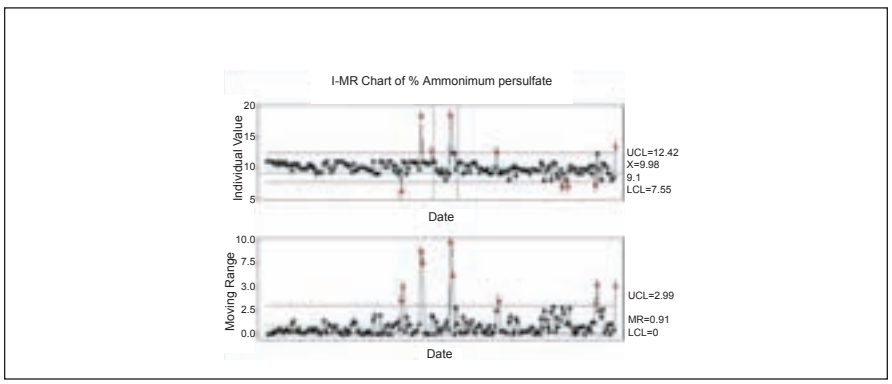

Figure 16—Run chart of ammonium persulfate concentration levels pre- and post-time of quality escape.

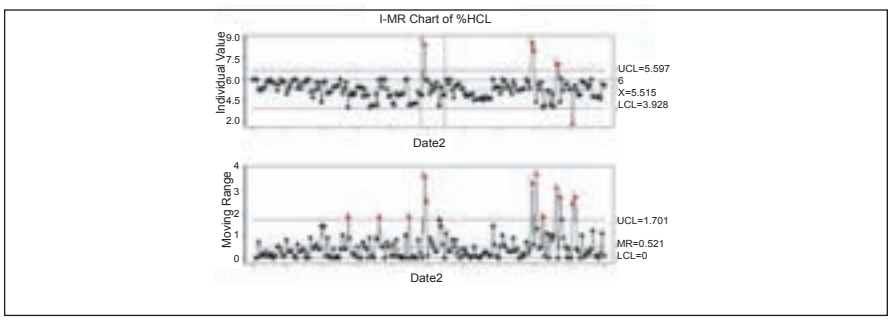

Figure 17—Run chart of HCL concentration levels pre- and post-quality escape time period.

Table 2 DOE Etch Process	
Step 1	Heat Specimen to 170˚ F for 3 mins.
Step 2	Blow dry.
Step 3	Immerse in enchant chemical 10.0 (min spec) secs.
Step 4	Rinse cold H_20.
Step 5	Heat specimen to 170˚ F for 1 min.
Step 6	Blow dry.
Step 7	Immerse in bleach solution 10.0 (max spec) secs.
Step 8	Rinse in cold H_20.
Step 9	Blow dry.

Gregory Blake *is a senior specialist, mechanical engineer, at Rolls Royce Corporation and holds the organizational position of product definition manager of gearboxes. Blake was granted a Bachelor of Science and a Master of Science degree from Purdue University. He has 15 years of professional experience in the areas of gear manufacturing, design, product development, and technology. He holds a special appointment to the Purdue University graduate school faculty. Blake was awarded the Rolls Royce Chief Executive Quality Award for Delivering Innovative Solutions and the Rolls Royce Executive Vice-Presidents Award for Customer Satisfaction. He has three patents for mechanical systems pending and has authored papers on the subjects of gear manufacturing, technology and failure analysis.*

Michael Margetts *is sub system design lead for the RB282-10 compressor. Prior, he was the structural analysis lead for the Transmissions and Structures group, primarily focused on the JSF Liftfan. Margetts has over 11 years of structural analysis experience which includes four years with Rolls Royce and seven years at General Electric. He completed his undergraduate degree at the Massachusetts Institute of Technology, following with graduate work at Tufts University in mechanical engineering.*

Wilson Silverthorne *currently serves as of Head of Engineering Quality & Improvement Programs for Rolls-Royce Corporation in Indianapolis, Indiana. Silverthorne joined Rolls-Royce in 2002 and previously held positions at Rolls-Royce in failure analysis, applications engineering and program engineering. He has over 15 years of engineering experience in the areas of metallurgy, gear heat treating and sintered friction material development. Silverthorne holds a BS in Materials Engineering from Purdue University, as well as an MBA from the University of Indianapolis. He is a special appointee to the Purdue University Graduate School faculty and has been awarded the Rolls Royce Executive Vice-President's Award for Customer Satisfaction and the Rolls-Royce Engineering and Technology Quality Award. He has authored and presented papers on various topics, including induction hardening and friction material technology.*

Table 3—DOE Test Matrix with Post Etch Results.

Test	Ammonium Persulfate %		HCl %		Detection of Etch Indications
1	18.6	Max	9.0	Max	↑
2	18.6	Max	3.0	Min	↑
3	6.0	Min	9.0	Max	→
4	6.0	Min	3.0	Min	→
5	9.1	Typical	6.0	Typical	↗
7	6.0	Min & min time	9.0	Max and max time	↘
8	6.0	Min & min time No glass bead	9.0	Max and max time	↓

and low test points. Table 3 details the concentration levels for each test. Further, the maximum and minimum time for exposure to the ammonium persulfate and HCL were tested.

The specimens were standard four-point bending specimens made from carburized AMS6265 material. The specimens were ground with aggressive parameters to induce surface temper.

Figure 17 shows the specimens, post processing. Each end of each specimen was etched separately, thus allowing for more test points. The use of both ends created an overlap area in the middle that must be excluded during final evaluation.

A qualitative scale was then created and the specimens evaluated by engineering. Table 3 contains the test matrix with the qualitative results.

An upward arrow indicates dark etch of tempered areas. The downward arrow indicates faint indications of the tempered area. The relative angle of the arrow is proportional to the degree of darkness of the etched indications.

Conclusions

- FEA and LEFM model predicted that crack would propagate across the tooth section.
- The grind etch DOE demonstrated that the ammonium persulfate process is robust and that concentration levels were adequate to detect grinding temper.
- Human factors are significant in non-destructive testing, such as etch inspection.

Recommendations for Future Work

- Additional data is needed to characterize the effects of the carburization on crack growth rate and trajectory.
- Processes should continue to be developed that minimize human factors in the detection of grinding abuse. ⚙

References

1. Parrish, G. "The Influence of Microstructure on the Properties of Case-Carburized Components," *American Society for Metals*, 1980, Materials Park, OH, Library of Congress Catalog No. 8010679.
2. American Gear Manufactures Association. "Surface Temper Etch Inspection After Grinding," 2007, AGMA 2007C00.
3. Lewicki, D. "Effects of Speed (Centrifugal Load) on Gear Crack Propagation Direction," 2001, U.S. Army Research Laboratory report number ARLTR1314.
4. Lewicki, D. "Gear Crack Propagation Path Studies—Guidelines for Ultra Safe Design," 2001, U.S. Army Research Laboratory report number ARLTR2468.
5. Blake, G. "The Effects of Super Finishing on Bending Fatigue," 2006, American Gear Manufactures Association, 06FTM.
6. Drago, R. *Fundamentals of Gear Design*, 1988, Butterworth Publishers, Stoneham, MA, ISBN 040990127.